Mechanical Technology and Engineering Insights

www.mtei.reapress.com

Mech. Technol. Eng. Insights. Vol. 3, No. 3 (2026) 216–225.

Paper Type: Original Article

Analytical and Three-Dimensional Finite Element Investigation of Multiaxial Loading on Stress Intensity Factor of U-Shaped Spot-Welded Joints

Omar Mar Cornelio[1,*], Hassan Masoomi[2]

[1] Department of Computational Mathematics, University of Computer Sciences, 19370 Havana, Cuba; omarmar@uci.cu.
[2] Department of Civil Engineering, University of California, Los Angles (UCLA), USA; masoomi.h@gmail.com.

Citation:

Received: 17 December 2025 *Revised: 26 February 2026* *Accepted: 14 April 2026*	Cornelio, O. M., & Masoomi, H. (2026). Analytical and three-dimensional finite element investigation of multiaxial loading on stress intensity factor of u-shaped spot-welded joints. *Mechanical Technology and Engineering Insights, 3*(3), 216-225.

Abstract

Resistance spot-welded joints are widely used in automotive structures and are often subjected to complex loading conditions that can lead to fatigue crack initiation and growth around the weld nugget. To evaluate the fracture-mechanics behaviour and structural integrity of these joints, accurate determination of Stress Intensity Factors (SIFs) is crucial. In the present study, the SIFs for a U-shaped resistance spot welded joint under multiaxial loading are investigated by three-dimensional Finite Element Analysis (FEA) and analytical approaches. We develop a detailed numerical model of the welded sheets and weld nugget in ABAQUS to characterise the local stress field and determine the corresponding SIFs. The numerical predictions are compared with those obtained from the analytical formulations proposed by Zhang and Swellam to assess their accuracy and applicability for the configuration investigated. In addition, the influence of weld nugget diameters and sheet thicknesses on the SIFs is studied systematically. The results show that Zhang's analytical model agrees better with the finite element predictions than Swellam's formulation for the loading and geometric conditions considered. In addition, the calculated SIFs increase with increasing weld nugget diameter and sheet thickness within the investigated parameter ranges. The results provide useful insight into the mixed-mode fracture behaviour of spot-welded joints and help to assess the validity of simplified analytical approaches for multiaxially loaded welded structures.

Keywords: Multiaxial loading, Mixed-mode fracture, Resistance spot welding, Finite element analysis, Stress intensity factor, Weld nugget diameter, Sheet thickness.

1 | Introduction

Resistance Spot Welding (RSW) is widely used in the automobile industry because it offers high production rates, relatively low cost, and the ability to join thin metal sheets. Spot-welded joints are exposed to complex combinations of tensile, shear, bending, and torsional loads in service. These loading conditions generate

Corresponding Author: omarmar@uci.cu
https://doi.org/10.48313/mtei.v3i3.90
Licensee System Analytics. This article is an open access article distributed under the terms and conditions of the Creative Commons Attribution (CC BY) license (http://creativecommons.org/licenses/by/4.0).

nonuniform stress fields around the weld nugget and may initiate and grow fatigue cracks. The weld nugget boundary is a geometrical discontinuity with a crack-like stress field. Fracture mechanics can effectively evaluate the fatigue performance and structural integrity of spot-welded joints.

In particular, Stress Intensity Factors (SIFs) are key fracture parameters that describe crack-tip behavior under opening (Mode I), sliding (Mode II), and tearing (Mode III) loading conditions [1–5].In particular, SIFs are important fracture parameters for characterizing crack-tip behavior under opening (Mode I), sliding (Mode II), and tearing (Mode III) loading conditions [1–5]. Early studies demonstrated the applicability of fracture mechanics to spot-weld fatigue assessment. Pook [1] investigated the fatigue behavior of spot welds using fracture mechanics concepts, and Radaj [2] investigated stress singularities, notch stresses, and structural stresses at spot-welded joints. Zhang [3] subsequently developed approximate analytical expressions to estimate SIFs and notch stresses in common spot-welded specimens and related these parameters to the applied loads and geometrical features.

Swellam et al. [4] studied SIFs in tensile-shear spot welds, adding further insight into the fracture behavior of these joints. Pan and Sheppard [5] studied SIFs in spot-welded structures, and Zhang and Taylor [6] investigated the effect of sheet thickness on fatigue behavior based on crack propagation. Together, these studies demonstrated the importance of joint geometry, loading configuration, and crack characteristics in determining the local fracture response. Further developments focused on analytical formulations that could simplify the evaluation of spot-welded joints under different loading conditions.

Lin and Pan [7] have developed closed-form solutions for the structural stresses and SIFs under various loading conditions. In their subsequent work [8], they generalized the solutions to the most commonly used specimen configurations, such as U-shaped, lap-shear, and cross-tension specimens. These formulations are useful alternatives to detailed numerical analysis, but their accuracy depends on the geometry, loading conditions, and assumptions of each model. Another way to evaluate the local stress field and investigate SIF variation around the weld nugget is three-dimensional Finite Element Analysis (FEA). Recent studies have also combined numerical simulation and data-driven techniques to predict the fatigue behavior of high-strength steel spot-welded joints [9]. Further studies have examined joint quality, fatigue resistance, and failure mechanisms in spot-welded and hybrid joints [10–14].

Meanwhile, research on fatigue in welded joints has investigated local-stress-based approaches, effective-notch-stress methods, and fatigue assessment procedures for different joint geometries and loading conditions [15–19]. Improvements in RSW processes have also been studied to improve electrode life and joint quality [20]. Although these studies offer insight into the general behavior of welded joints, they do not eliminate the need to validate analytical SIF formulations for specific spot-weld configurations.

In particular, the relative accuracy of the Zhang and Swellam models for a U-shaped spot-welded joint subjected to multiaxial loading needs to be systematically evaluated. Further study is also warranted on how weld nugget diameter and sheet thickness affect the calculated SIFs and the agreement between analytical and numerical predictions. Thus, the present study investigates the SIFs of a U-shaped resistance spot-welded joint under multiaxial loading using three-dimensional FEA in ABAQUS. The numerical results are compared to the analytical predictions from the Zhang and Swellam formulations to assess their relative accuracy under the conditions considered.

In addition, parametric studies are conducted to investigate the influence of the weld nugget diameter and the sheet thickness on the fracture-mechanics response. The main contribution of this work is a comparative evaluation of the two analytical models against three-dimensional finite element results for the investigated joint configuration, along with an assessment of the influence of key geometric parameters. The results are aimed at clarifying the applicability of simplified analytical approaches for engineering analysis of spot-welded joints under combined loading conditions.

2 | Analytical Methods

Numerous researchers have developed analytical methods to determine the SIFs for resistance spot-welded joints, including the models of Swellam et al. [4] and Zhang [3]. In the present study, these two formulations are independently used to evaluate the SIFs of a U-shaped spot-welded joint under combined tensile and shear loading. The specimen geometry and the dimensional parameters of interest are sketched in *Fig. 1*.

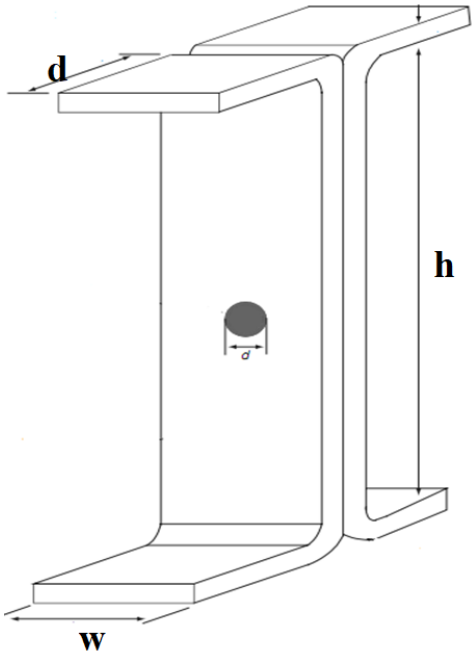


Fig. 1. Geometry and dimensions of the U-shaped spot-welded specimen.

2.1 | Swellam Model

Swellam et al. [4] proposed a combined fracture parameter based on the weld nugget's geometric characteristics and the applied loading components. In this approach, the spot-welded joint is idealized as two elastic half-spaces joined over a circular region representing the weld nugget. The joint can be subjected to tensile force, bending moment, and shear force. This leads to mixed-mode fracture involving modes I and II. The combined parameter considers the contributions of the corresponding SIFs and provides a way to characterize the fracture response under combined loading. *Eqs. (1)–(3)* are analytical expressions proposed by Swellam et al. [4].

$$K_I = \frac{P}{2r\sqrt{\pi r}} + \frac{3M}{2r^2\sqrt{\pi r}}. \quad (1)$$

$$K_{II} = \frac{Q}{2r\sqrt{\pi r}}\acute{y}. \quad (2)$$

$$K_{eq} = \sqrt{{K_I}^2 + {K_{II}}^2}. \quad (3)$$

Here, (r) is the weld nugget radius, (P_z) is the normal component of the applied force, (P_x) is the shear force, and (M) is the bending moment at the weld nugget center. The stress intensity factor equivalent is found by adding the contributions of the relevant fracture modes as per the original formulation. *Fig. 2*. Force and moment components at the center of the weld nugget for a general loading configuration.

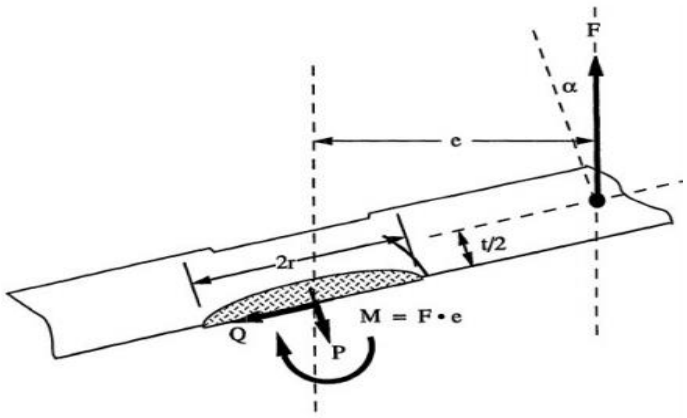


Fig. 2. Schematic representation of the applied force components and bending moment at the center of the weld nugget under combined tensile and shear loading.

2.2 | Zhang Model

Zhang [4] derived analytical expressions to calculate the SIFs at the critical locations around the weld nugget based on the applied loads and the geometric features of the welded specimen. Unlike a formulation that is primarily based on the local loading components, Zhang's formulation accounts for specimen-specific geometric parameters. It allows for estimation of the SIFs for different spot-welded configurations. The SIFs for the U-shaped specimen considered in this paper have been calculated using the relations proposed by Zhang, as shown in *Eq. (4)*. In these expressions, (P_t) and (P_s) are the applied tensile and shear forces, respectively; (L) is the specimen length; (d) is the weld nugget diameter; and (t) is the sheet thickness. The parameter (f) accounts for the specimen width and is assumed to take the values given in *Table 1* [4].

Table 1 . Geometric correction factor ( ) in Zhang's analytical model [4].

$\mathbf{e = \frac{(w - d)}{2}}$					
Specimen Width-to-Length Parameter $\frac{e}{d}$	1.0	1.5	2.0	2.5	3.0
η	1.68	1.47	1.26	1.06	0.94

Then, the SIFs obtained from the Zhang formulation are compared with those calculated by the Swellam model and three-dimensional FEA. This comparison is used to judge the relative accuracy of two analytical approaches for the investigated joint geometry and loading conditions.

3 | Finite Element Method Analysis

The Finite Element Method (FEM) is widely employed to evaluate SIFs in spot-welded joints. The numerical results depend heavily on the weld geometry representation, applied boundary conditions, element formulation, and mesh refinement around the weld nugget and crack tip. Reliable SIF calculations depend on an appropriate mesh and fracture mechanics formulation because of the stress-field behavior near the crack tip. In this study, we developed a three-dimensional finite element model in Abaqus to study the SIFs of a U-shaped spot-welded specimen under combined tensile and shear loading. The model was used to investigate the local stress field around the weld nugget and to derive SIFs for the different fracture modes.

3.1 | Geometry Modelling and Mesh Generation

The sheet components and the weld nugget were modelled as three-dimensional solid geometry. The weld nugget was modelled as a cylinder with the radius of the weld radius and the height of two times the sheet thickness.

The geometric representation of the weld nugget and the corresponding finite element model are depicted in *Figs. 3* and *4a*, respectively. We generated a refined finite element mesh around the weld nugget and crack area to improve the accuracy of the calculated fracture parameters. The model contained 25,071 quadratic hexahedral elements of type C3D20R. The elements were 20-node three-dimensional solid elements with reduced integration and were used to discretise both the base metal and the weld nugget. The specimen material was SAE 1010 steel. The same material properties were assigned to the base metal and the weld nugget, since the welding thermal cycle's effect on local mechanical properties was not considered. A summary of the mechanical properties used in the simulations is presented in *Table 2*.

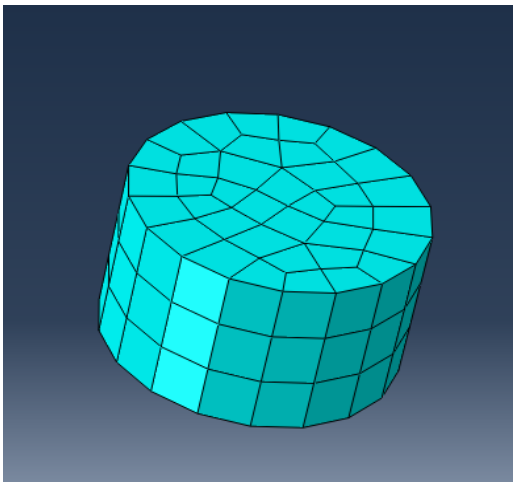


Fig. 3. Photograph of the spot-weld nugget.

Table 2. Mechanical properties of SAE 1010 steel.

Property	Symbol	Value
Young's modulus	E(GPa)	210
Poisson's ratio	υ	0.30
Yield strength or tensile strength	S_u(MPa)	331
Density	S_y(MPa)	210

3.2 | Boundary Conditions and Loads

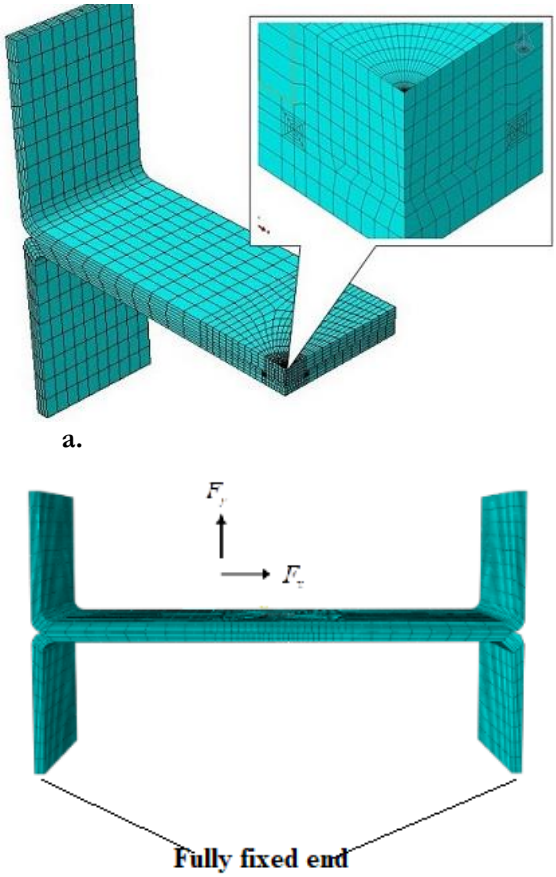
The boundary conditions were set up to simulate the mechanical loading of the U-shaped spot-welded specimen. The bottom surface of the lower sheet was constrained to prevent rigid-body motion. Tensile and shear loads were applied at a reference point, and the loading configuration is shown in *Fig. 4b*. The response of the welded joint under combined loading was investigated using the applied loads.

Then, the stress distribution around the weld nugget was analyzed to find out the corresponding fracture parameters. The loading directions, reference-point coupling constraints, and restrained degrees of freedom were defined according to the numerical model.

3.3 | Stress analysis and calculation of SIFs

The SIFs were extracted using Abaqus' contour integral technique. After dividing the area around the weld nugget, we defined the crack location and propagation path along the sheet thickness. A crack-tip singularity parameter of 0.25 was assumed in the numerical model. The crack-tip mesh and singularity definition represented the local stress field required to evaluate fracture parameters. The SIFs for the fracture modes considered in this study were evaluated using the contour integral method.

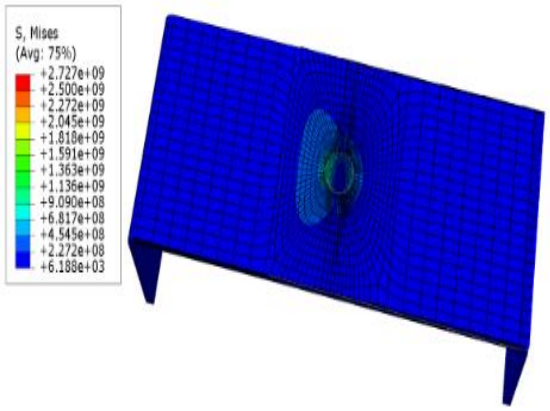
In particular, the mode-I and mode-II SIFs (K_I) and (K_{II}) were used to characterize the response under tensile and shear loading, respectively. We tested the robustness of the extracted values by examining how the calculated SIFs varied across successive contours and, when available, by performing a mesh-refinement study. The fine mesh around the weld nugget and crack region increased the analysis cost. For example, a simulation with an applied load of 500 N took approximately 8 h of computational time. *Fig. 5* shows the stress contours and the local crack-tip region in *Fig. 5a* and *Fig. 5b*, respectively.



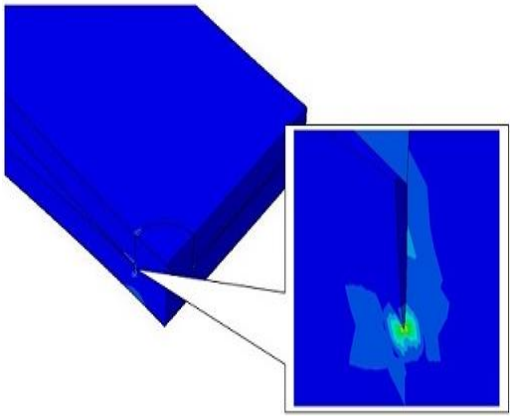
a.

b.

Fig. 4 Finite element model and boundary conditions of U-shaped spot-welded specimen; a. finite element mesh and geometric partitioning; b. boundary conditions and applied loads, with the bottom end fully fixed.



a.



b.

Fig. 5. a. Stress contours in the spot-welded specimen; b. Local singular field around the modelled crack.

4 | Results and Discussion

In this respect, the Swellam formulation accounts for the weld nugget diameter *Eqs. (1)* and *(2)*, while the Zhang model considers both the nugget diameter and the sheet thickness. The analytical formulations and FEA were employed to calculate the mode-I and mode-II SIFs for different nugget diameters and sheet thicknesses to investigate the influence of these geometric parameters. The tensile and shear loads were 500 N each for all the simulations. The corresponding results are shown in *Table 3*. It is found that the diameter of the weld nugget and the sheet thickness have strong effects on the SIFs. With the increase of the nugget diameter for the same sheet thickness, the SIFs for modes I and II are generally decreased. This behavior can be explained by the redistribution of applied loads over a larger welded region, reducing stress concentration at the weld-nugget boundary.

Similarly, for a given nugget diameter, the SIFs decrease as sheet thickness increases, as the joint becomes stiffer. The comparison between the analytical and finite element results highlights differences in the accuracy of the two formulations. The numerical results for the investigated geometric configurations show that the Zhang model agrees relatively well with the numerical results. The deviation is larger for the Swellam model, especially for larger nugget diameters. *Fig. 6* shows the ratio of the analytically predicted SIFs to the corresponding finite element values as a function of the nugget diameter-to-sheet-thickness ratio, d/t, further to evaluate the predictive capability of the analytical formulations. A ratio of 1 means the analytical and numerical predictions agree perfectly.

Table 3. SIFs obtained from FEA and analytical models.

Case	d (mm)	t (mm)	FEA KI	FEA KII	Zhang KI	Zhang KII	Swellam KI	Swellam KII
1	4	1	1105.94	53.3	1139.91	56.27	981.79	35.26
2	4	1.3	753.56	47.49	762.3	49.35	—	—
3	4	1.6	531.34	41.658	558.395	44.485	—	—
4	5.4	1	819.287	39.2	841.136	41.68	596.98	22.48
5	5.4	1.3	541.54	33.67	553.98	36.55	—	—
6	5.4	1.6	398.32	30.99	405.73	33.95	—	—
7	8	1	512.39	40.04	534.41	41.68	227.54	12.46
8	8	1.3	361.54	31.78	373.94	34.67	—	—
9	8	1.6	259	22.02	264.058	22.24	—	—

The Zhang predictions in *Fig. 6* are close to unity, indicating good agreement with the finite element results. Conversely, the Swellam prediction decays substantially compared with the numerical results as the diameter-to-thickness ratio increases. This trend indicates that the Swellam formulation is less accurate for the larger nugget diameters considered in the present study.

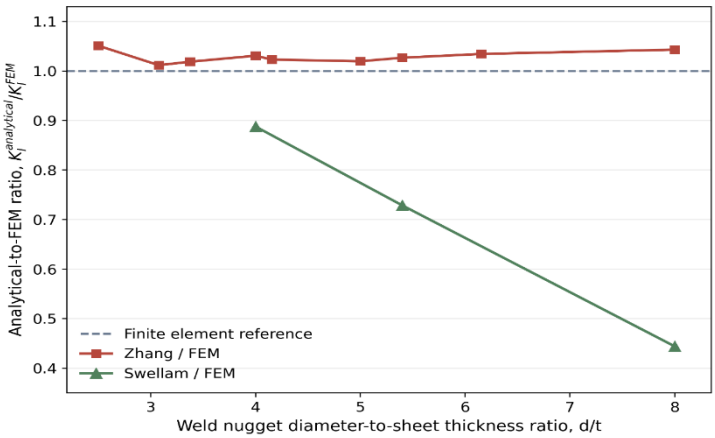


Fig. 6. Comparison of the analytical-to-numerical stress intensity factor ratios predicted by the Zhang and Swellam models as a function of the weld nugget diameter-to-sheet thickness ratio (d/t).

Overall, the comparison shows that the Zhang formulation provides a more reliable approximation of the SIFs for the analyzed U-shaped spot-welded joint. The better agreement with the finite element results underlines the importance of the relevant geometric parameters in evaluating the fracture behavior of spot-welded structures.

5 | Conclusion

In this study, the SIFs of a U-shaped spot-welded joint under combined tensile and shear loading were investigated using three-dimensional FEA and the analytical formulations proposed by Zhang and Swellam. The effects of weld nugget diameter and sheet thickness on the mode-I and mode-II SIFs were investigated. Based on the results, the following conclusions can be made:

I. The weld nugget diameter and sheet thickness have a significant influence on the fracture behavior of the spot-welded joint. The SIFs are generally reduced with the increase of both parameters, which indicates a lower crack tip stress concentration for the studied loading conditions.

II. The Zhang formula shows good agreement with the finite element results for all the geometric configurations studied. However, the Swellam model shows larger deviations, especially as the weld nugget diameter increases.

III. The ratios of analytical to numerical SIFs are compared. It is found that the Zhang model gives more consistent results, and the Swellam model underestimates the numerical results for larger diameter-to-thickness ratios.

IV. The enhanced performance of the Zhang formulation demonstrates the importance of considering both weld nugget diameter and sheet thickness for the evaluation of the SIFs of U-shaped spot-welded joints.

Overall, the results indicate that the Zhang formulation provides a better analytical approach for estimating SIFs for the joint geometry and loading conditions considered in this study. These results provide useful insight into how geometric parameters influence the fracture response of spot-welded structures.

Conflict of Interest

The authors declare no conflict of interest.

Data Availability

All data are included in the text.

Funding

This research received no specific grant from funding agencies in the public, commercial, or not-for-profit sectors.

Refrences

[1] Pook, L. P. (1975). Fracture mechanics analysis of the fatigue behaviour of spot welds. *International Journal of Fracture*, *11*(1), 173-176. https://doi.org/10.1007/BF00034726

[2] Radaj, D. (1989). Stress singularity, notch stress and structural stress at spot-welded joints. *Engineering fracture mechanics*, *34*(2), 495-506. https://doi.org/10.1016/0013-7944(89)90161-6

[3] Zhang, S. (1999). Approximate stress intensity factors and notch stresses for common spot-welded specimens. *Welding journal-New York*, *78*, 173-179. https://s3.us-east-1.amazonaws.com/WJ-www.aws.org/supplement/WJ_1999_05_s173.pdf

[4] Swellam, M. H., Ahmad, M. F., Dodds, R. H., & Lawrence, F. V. (1992). The stress intensity factors of tensile-shear spot welds. *Computing systems in engineering*, *3*(1-4), 487-500. https://doi.org/10.1016/0956-0521(92)90134-5

[5] Pan, N., & Sheppard, S. D. (2002). Stress intensity factors in spot welds. *Engineering fracture mechanics*, *70*(5), 671-684. https://doi.org/10.1016/S0013-7944(02)00076-0

[6] Zhang, Y., & Taylor, D. (2000). Sheet thickness effect of spot welds based on crack propagation. *Engineering fracture mechanics*, *67*(1), 55-63. https://doi.org/10.1016/S0013-7944(00)00029-1

[7] Lin, P. C., & Pan, J. (2008). Closed-form structural stress and stress intensity factor solutions for spot welds under various types of loading conditions. *International journal of solids and structures*, *45*(14-15), 3996-4020. https://doi.org/10.1016/j.ijsolstr.2008.02.006

[8] Lin, P. C., & Pan, J. (2008). Closed-form structural stress and stress intensity factor solutions for spot welds in commonly used specimens. *Engineering fracture mechanics*, *75*(18), 5187-5206. https://doi.org/10.1016/j.engfracmech.2008.08.005

[9] Yu, Z., Ma, N., Murakawa, H., Watanabe, G., Liu, M., & Ma, Y. (2023). Prediction of the fatigue curve of high-strength steel resistance spot welding joints by finite element analysis and machine learning. *The international journal of advanced manufacturing technology*, *128*(5), 2763-2779. https://doi.org/10.1007/s00170-023-11993-y

[10] Santos, J. I., Martín, Ó., Ahedo, V., de Tiedra, P., & Galán, J. M. (2022). Glass-box modeling for quality assessment of resistance spot welding joints in industrial applications. *The international journal of advanced manufacturing technology*, *123*(11), 4077-4092. https://doi.org/10.1007/s00170-022-10444-4

[11] Heidrich, D., Zhang, F., & Fang, X. (2021). Fatigue strength of rivet resistance spot welding technique in comparison with self-piercing riveting for multi-material body-in-white structure. *Journal of materials engineering and performance*, *30*(5), 3806-3821. https://doi.org/10.1007/s11665-021-05684-6

[12] Meilinger, Á., Cserépi, M. F., & Lukács, J. (2024). Behaviour of aluminium/steel hybrid RSW joints under high cycle fatigue loading. *Welding in the world*, *68*(2), 427-440. https://doi.org/10.1007/s40194-023-01663-8

[13] Prabitz, K. M., Antretter, T., Rethmeier, M., El-Sari, B., Schubert, H., Hilpert, B., ... & Ecker, W. (2024). Numerical and experimental assessment of liquid metal embrittlement in externally loaded spot welds. *Welding in the world*, *68*(10), 2713-2722. https://doi.org/10.1007/s40194-024-01696-7

[14] Ullrich, M., Wohner, M., & Jüttner, S. (2024). Quality monitoring for a resistance spot weld process of galvanized dual-phase steel based on the electrode displacement. *Welding in the world*, *68*(7), 1791-1800. https://doi.org/10.1007/s40194-024-01720-w

[15] Lippardt, S. (2023). Influence of the geometry on the fatigue strength of welded joints using the effective notch stress approach. *Welding in the world*, *67*(3), 669-681. https://doi.org/10.1007/s40194-022-01409-y

[16] Zanetti, M., Babini, V., & Meneghetti, G. (2021). Fat classes of welded steel details derived from the master design curve of the peak stress method. *Welding in the world*, *65*(4), 653-665. https://doi.org/10.1007/s40194-020-01057-0

[17] Rudorffer, W., Wächter, M., Esderts, A., Dittmann, F., & Varfolomeev, I. (2022). Fatigue assessment of weld seams considering elastic–plastic material behavior using the local strain approach. *Welding in the world*, *66*(4), 721-730. https://doi.org/10.1007/s40194-021-01242-9

[18] Scacco, F., Zerbst, U., Meneghetti, G., & Madia, M. (2022). Comparison between PSM and IBESS approaches for the fatigue life estimation of weldments. *Welding in the world*, *66*(6), 1251-1273. https://doi.org/10.1007/s40194-022-01284-7

[19] Yoshihara, Y., Osawa, N., Murakawa, H., & Dai, P. (2025). Study on the estimation method for the mean stress effect on the fatigue strength of welded joints with various failure modes and joint types. *Welding in the world*, *69*(1), 151-167. https://doi.org/10.1007/s40194-024-01815-4

[20] Brechelt, S., Wiche, H., Junge, J., Gustus, R., Schmidt, H., & Wesling, V. (2023). Increase of electrode life in resistance spot welding of aluminum alloys by the combination of surface patterning and thin-film diffusion barriers. *Welding in the world*, *67*(12), 2703-2714. https://doi.org/10.1007/s40194-023-01614-3

Appendix

Table A1. Nomenclature of mechanical and fracture mechanics parameters.

No.	Parameter	Symbol
1	Specimen length	b
2	Young's modulus	E
3	Weld nugget diameter	d
4	Mode I and Mode II stress intensity factors	(K_I,K_{II})
5	Bending moment	M
6	Tensile force	P
7	Shear force	V
8	Weld nugget radius	r
9	Yield strength	s_y
10	Ultimate tensile strength	s_u
11	Base sheet thickness	t
Greek Symbols		
1	Specimen width correction factor	η
2	Poisson's ratio	υ